J|A|C|S COMMUNICATIONS

Published on Web 07/30/2010

A Highly Selective Low-Background Fluorescent Imaging Agent for Nitric Oxide

Youjun Yang,[†] Stephanie K. Seidlits,[‡] Michelle M. Adams,[†] Vincent M. Lynch,[†] Christine E. Schmidt,[‡] Eric V. Anslyn,*[,†] and Jason B. Shear*[,†,§]

Department of Chemistry and Biochemistry, Department of Biomedical Engineering, and Institute for Cellular and Molecular Biology, University of Texas at Austin, Austin, Texas 78712

Received May 10, 2010; E-mail: anslyn@austin.utexas.edu

Abstract: We introduce a novel sensing mechanism for nitric oxide (NO) detection with a particular easily synthesized embodiment (NO_{550}), which displays a rapid and linear response to NO with a red-shifted 1500-fold turn-on signal from a dark background. Excellent selectivity was observed against other reactive oxygen/nitrogen species, pH, and various substances that interfere with existing probes. NO_{550} crosses cell membranes but not nuclear membranes and is suitable for both intra- and extracellular NO quantifications. Good cytocompatibility was found during in vitro studies with two different cell lines. The high specificity, dark background, facile synthesis, and low pH dependence make NO_{550} a superior probe for NO detection when used as an imaging agent.

The biological roles of nitric oxide (NO) have led chemists and molecular biologists to seek cellular imaging agents responsive to this species. Interest in such agents derives from the pivotal role of NO in vasodilation as an endothelial-derived relaxing factor (EDRF); its function as a platelet aggregation inhibitor, neurotransmitter, and antimicrobial agent; and its antitumor activity in cardiovascular, nervous, and immune systems.[1,2] Although a variety of quantification techniques have been developed, fluorescence techniques have become the gold standard for NO sensing because of their sensitivity and high spatiotemporal resolution when combined with microscopy.[3,4]

A number of fluorescent NO probes have been reported to date.[5−15] The most common approach for NO detection involves the use of *o*-diamino aromatics under aerobic conditions. These species react with NO^+, or N_2O_3, to furnish fluorescent triazole derivatives.[5,6,8−10] Turn-on fluorescence signals are achieved through suppression of photoinduced electron transfer (PET). Examples using fluoresceins[5] (such as DAF-2 DA, Scheme 1), anthraquinones,[6] rhodamines[8,13] (such as DAR-4M AM), BODIPYs,[9] and cyanines[10] have been documented. Such probes are among the current state of the art, yet limitations exist. First of all, in the presence of H_2O_2/peroxidase, $OONO^-$, $OH^•$, $NO_2^•$, or $CO_3^{•-}$, the intrinsically electron-rich diaminobenzene moiety is oxidized to an arylaminyl radical, which combines with NO and leads to triazoles.[16−18] Second, dehydroascorbic acid (DHA) condenses with *o*-diamino aromatics and turns on the fluorescence of such probes.[19] It has been reported that 1 mM DHA yields fluorescence signals with the commercial NO probes DAF-2 DA and DAR-4M AM that are comparable to those for 300 nM and 100 μM NO, respectively.[20] Third, benzotriazoles are pH-sensitive near neutral pH ($pK_a \approx 6.7$).[8,20] The aforementioned limitations complicate NO detection using *o*-diamines. Hence, a series of metal−ligand complexes[11,12,21] and single-walled carbon nanotubes[15] for NO detection are under development.

Scheme 1. A Representative NO Probe and Its Detection Mechanism

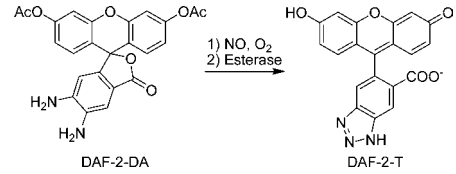

We sought to overcome the limitations of the *o*-diamino aromatics by creating a chemical mechanism for NO detection that eliminates the possibility of interferences, thereby rendering very high specificity. Herein, we report the design and synthesis of a highly selective NO-responsive fluorescent probe based on this new strategy, evaluate its spectroscopic attributes, and demonstrate its application in cellular imaging.

We reasoned that very high specificity for NO could be achieved if the chromophore/fluorophore of the probe is not assembled until the assembly process is triggered by the unique reactivity of NO. Moreover, an increase in conjugation would be expected to yield an advantageous red-shifted turn-on signal. We also avoided the highly electron-rich *o*-diamino aromatics in order to impede general oxidation by other reactive oxygen/nitrogen species and avoid condensation with ascorbic acid (AA) analogues. Our strategy involves a cascade of reactions that commence from air oxidation of NO. Our first embodiment of the strategy was the probe NO_{550}, which upon reaction with NO was predicted to generate a diazo ring system (AZO_{550}, Scheme 2). The dimethylamino and cyano groups were judiciously positioned to allow internal charge transfer upon photoexcitation. A short, simple two-step synthesis produces NO_{550} in an overall yield of 90%.

Scheme 2. Probe NO_{550} and the Proposed Stepwise Route to AZO_{550}

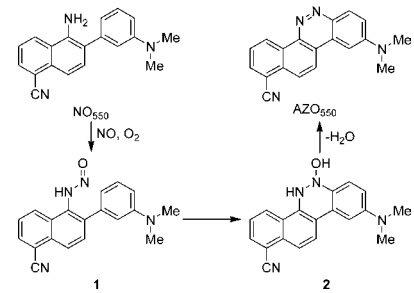

Our first studies involved bubbling NO gas into a solution of NO_{550} in CH_2Cl_2. A color change from light-yellow to deep-red was immediately observed. This phenomenon qualitatively demonstrated that NO_{550} is reactive toward NO/N_2O_3, and the structure of the product (AZO_{550}) was unambiguously established using NMR spectroscopy, mass spectrometry, and X-ray crystallography (Figure S1 and Table S1 in the Supporting Information). The ring closure occurs para to the dimethylamino group rather than ortho, presumably because of steric hindrance.

[†] Department of Chemistry and Biochemistry.
[‡] Department of Biomedical Engineering.
[§] Institute for Cellular and Molecular Biology.

10.1021/ja1040013

The reaction between NO_{550} and NO requires NO^+ or an NO^+ donor such as N_2O_3.[5] The reaction resembles the synthesis of azo compounds via a diazotization/coupling sequence. However, a profound difference exists. Diazotization occurs in acidic media to form diazonium salts from nitrosamines. In contrast, the reaction between NO_{550} and NO occurs rapidly under neutral (pH 7.4, see below) or even basic (pH = 10; Figure S2) aqueous conditions, where conversion of the initially formed nitrosamine derivative (**1**) to the corresponding diazonium salt via acid-catalyzed dehydration is unlikely. This implies that electrophilic aromatic substitution on the electron-deficient nitrosamine occurs, yielding a hydroxyhydrazine derivative (**2**). Elimination of H_2O would lead to the formation of AZO_{550}.

Because of the limited aqueous solubility of NO_{550}, 20% DMSO in PBS buffer (50 mM at pH 7.4 with 150 mM NaCl) was used for spectroscopic studies. NO_{550} displays an absorption band centered at 352 nm that tails to 450 nm (Figure S3) and shows minimal fluorescence in this solvent, likely as a result of a combination of PET from the 3′-dimethylaminophenyl ring and rotational deactivation along the aryl−aryl single bond. As an aliquot of the NO stock solution (1.9 mM in deionized H_2O[22]) was added, an absorption band centered at 450 nm appeared immediately while the band at 352 nm diminished. The large bathochromic shift enables selective photoexcitation of AZO_{550} and eliminates any undesired background fluorescence from the unreacted probe. Concomitantly, an emission band centered at 550 nm (with a broad maximum excitation ranging from 440 to 470 nm) appeared from a dark background (Figure 1A). The spectra were identical to those for purified AZO_{550}. A dark background from which a bright signal appears in response to NO is unique to our strategy and advantageous in comparison with other existing probes. Standard fluorescein filter sets match with the spectral properties of AZO_{550} and can be used for NO imaging, as exemplified below. A fluorescence enhancement of over 1500-fold (Figure S4) was observed, which can be compared with the ∼200-fold enhancement with DAF-2 (calculated on the basis of published photophysical parameters[5]). An excellent linear correlation ($R^2 = 0.997$) between the fluorescence enhancement and the NO concentration was found (Figure 1B). The kinetics of the reaction of NO_{550} with NO was studied using time-based fluorescence (λ_{ex} = 470 nm, λ_{em} = 550 nm). The kinetics of signal production appears to be multiexponential, but the fast phase of signal generation (>80% of the total signal) is complete within ∼20s (Figure 1C). This fast kinetic profile allows for good temporal resolution in cellular imaging studies. Unlike the existing fluorescein-based probes, the fluorescence of AZO_{550} is completely independent of pH over the range 4.5−9 (Figure S5), which is advantageous because different cells, or different compartments in the same cell, may have different pH values. The molar absorptivity at 470 nm and the fluorescence quantum yield of AZO_{550} were 4000 M^{-1} cm^{-1} and 0.11, respectively, in 20% DMSO. The limit of detection (LOD), the point at which the signal equals three times the noise, was estimated to be ∼30 nM in 20% DMSO (Figure 1B). We screened a wide array of possible competitive reactive oxygen or nitrogen species and other analytes at up to 1000-fold excess: H_2O_2, NO_3^-, NO_2^-, AA, DHA, ClO^-, $O_2^{\bullet-}$, $OH^\bullet$, O_3, $^1O_2$, and $ONOO^-$. No detectable signal for any of these analytes above a blank was obtained (Figure S8). The very high selectivity for NO is due to our unique detection mechanism.

NO_{550} was used to visualize both endogenously produced NO and NO exogenously supplied by a donor (sodium nitroprosside, SNP) in cultures of two cell types: neonatal spinal astrocytes and the pheochromocytoma-derived PC12 cell line, which is commonly used as a model for neurons. Both cell types have previously been reported to produce NO.[19,23] NO_{550} appears to enter the cytoplasm in both cell types but does not cross into the nuclei. The viability of the astrocytes and PC12 cells upon incubation with the NO dye was evaluated by measuring their metabolic activity after 30 min. No differences were observed between cells incubated with the probe and controls (Figure S6).

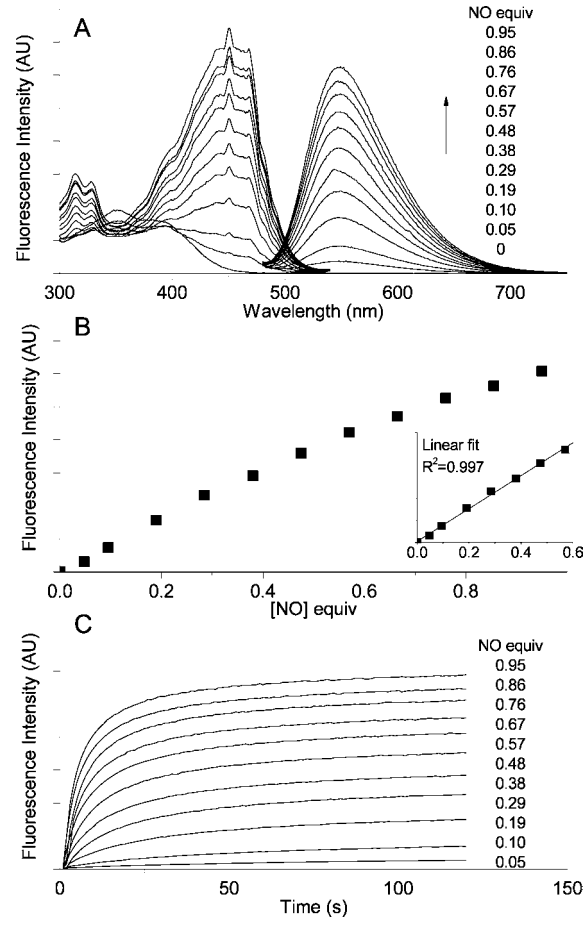

Figure 1. Spectroscopic studies of NO sensing using NO_{550}. (A) Overlay of the excitation spectra (λ_{em} = 550 nm) and emission spectra (λ_{ex} = 470 nm) obtained when different aliquots of NO were added to an NO_{550} solution (50 μM) in PBS buffer containing 20% DMSO. Spectra were collected 2 min after NO addition. (B) Enhancement of the fluorescence intensity (λ_{ex} = 470 nm, λ_{em} = 550 nm) upon NO addition over a period of 2 min. (C) Kinetic profiles of the reaction between NO_{550} and NO (λ_{ex} = 470 nm, λ_{em} = 550 nm).

We performed several in vitro experiments to confirm that NO_{550} responds to NO in a biological context. Astrocytes were stimulated with interleukin-1β (IL-1β) and interferon-γ (IFN-γ) to induce NO production and then incubated with NO_{550} for 15 min. A stronger fluorescence signal was observed for astrocytes displaying the "spindle" phenotype, which is induced by cytokine stimulation and exhibits a rounded cell body and spindle-like projections, than for those exhibiting a flattened, spread phenotype (Figure 2A). This agrees with previous reports that the spindle phenotype produces higher levels of NO when induced by cytokines.[23,24] Longer incubation times (>15 min) with NO_{550} did not lead to enhanced fluorescence, indicating that the probe had reached a diffusive equilibrium in the cells. As a negative control, when NO_{550} was incubated with astrocytes not stimulated to produce NO, a substantially weaker fluorescence signal was observed (Figure S9). This result is further evidence that NO_{550} reacts with cellularly produced NO. Upon addition of SNP to cell cultures, a notable increase in fluorescence of both astrocytic phenotypes occurred (Figure 2B; data with PC12 cells not shown). Line scans were taken through the center (x axis) of the images for quantitative comparison, and the data from Figure 2A,B showed a measurably larger fluorescence increase when SNP was added to the cell culture (Figure 2E).

We also compared NO_{550} to a commercially available NO probe, DAF-2 DA (Figure 2C,D). Quantitative analysis showed that NO_{550}

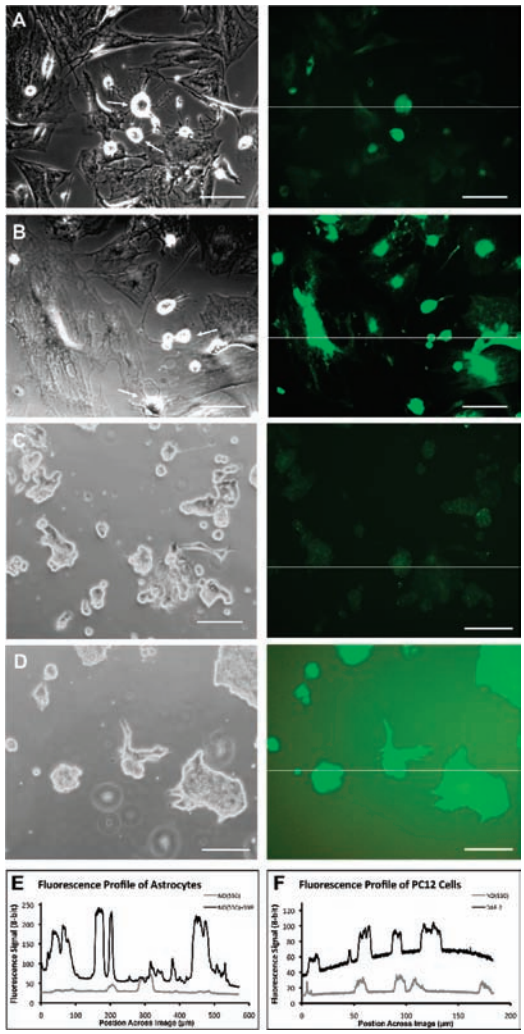

Figure 2. Fluorescence imaging of NO in live cell cultures. (A) Phase-contrast image (left) and corresponding wide-field fluorescence image (right) of neonatal spinal astrocytes stimulated with IFN-γ and IL-1β and incubated with 10 μM NO_{550}. In the phase contrast-images, bright edges indicate presence of intact cell membranes, with brighter areas indicating where the membrane is thicker. (B) Same imaging sequence as in (A) for astrocytes treated identically to those in (A) except that 1 mM SNP was added. The small arrows in (A) and (B) indicate astrocytes exhibiting a cytokine-induced phenotype characterized by spindle-like projections and increased NO expression. (C) Same imaging sequence as in (A) for NGF-stimulated PC12 cells incubated with 10 μM NO_{550}. (D) Same imaging sequence as in (A) for NGF-stimulated PC12 cells incubated with 10 μM DAF-2 DA. Scale bars = 150 μm. Linear levels were adjusted in all images using Adobe Photoshop to aid in visualization. Brighter areas indicate areas where the membrane is thicker. (E) Plots of fluorescence signal, as measured along the dotted lines, from the raw images of astrocytes in (A) and (B). (F) Plots of fluorescence signal from raw images of PC12 cells in (C) and (D). Fluorescence was obtained using a fluorescein filter set with excitation 450−490 nm and emission 520 nm long-pass filters.

(10 μM) yielded a higher ratio of signal (i.e., fluorescence within cells) to background (here, the extracellular fluorescence) than DAF-2 DA (10 μM) upon incubation with PC12 cells (Figure 2F). The majority of the extracellular background fluorescence signal most likely resulted from side reactions with extracellular species such as DHA.[20] However, signal from thermally cleaved dye and even uncleaved dye (autofluorescence) also may have contributed. An even higher background was observed when DAR-4M AM was used (data not shown), in agreement with its elevated reactivity toward DHA relative to DAF-2 DA. In addition, a concentration of NO_{550} up to 50 μM could be used to further increase the signal without increasing the background in the images (Figure S7). In contrast, higher signal intensity was not observed when a higher concentration of DAF-2 DA (up to 50 μM) was applied (data not shown). NO_{550} was not observed to permeate the nuclear membrane, while fluorescence was observed in the cell nuclei in cultures incubated with DAF-2 DA. The fluorescence signal from NO_{550} was concentrated around the nuclei upon incubation with both cell lines. This further confirms the utility of NO_{550}, as NO synthase associates with the Golgi bodies near the nucleus in both cytokine-stimulated astrocytes and nerve growth factor (NGF)-stimulated PC12 cells.[24,25] Thus, it is reasonable to expect that more NO is present in these high-density areas of NO synthase.

In summary, quantitative NO measurement via fluorimetry is a challenging task because of the lack of probes that display high specificity. We have introduced a novel mechanism for NO detection with a particular easily synthesized embodiment (NO_{550}), which displays a rapid and linear response to NO with a red-shifted 1500-fold turn-on signal from a dark background. Excellent selectivity was observed against other reactive oxygen/nitrogen species, pH, and various substances that interfere with the existing probes. The probe is suitable for both intra- and extracellular NO imaging. The high specificity, dark background, facile synthesis, and low pH dependence make NO_{550} a superior probe for NO detection when used as an imaging agent.

Acknowledgment. We are grateful for support from the National Science Foundation through Grant CHE-0716049 and the Welch Foundation through Grant F-1331. J.B.S. is a Fellow in the Institute for Cellular and Molecular Biology. The purchase of a diffractometer was funded by the National Science Foundation through Grant 0741973.

Supporting Information Available: Synthesis and compound characterizations, CIF file and ORTEP drawing of AZO_{550}, and additional spectroscopic and cellular imaging studies using NO_{550}. This material is available free of charge via the Internet at http://pubs.acs.org.

References

(1) *Nitric Oxide*; Mayer, B., Ed.; Handbook of Experimental Pharmacology, Vol. 143; Springer: Berlin, 2000.
(2) *Nitric Oxide Biology and Pathobiology*; Ignarro, L. J., Ed.; Academic Press: San Diego, CA, 2000.
(3) Nagano, T.; Yoshimura, T. *Chem. Rev.* **2002**, *102*, 1235.
(4) Hetrick, E. M.; Schoenfisch, M. H. *Annu. Rev. Anal. Chem.* **2009**, *2*, 409.
(5) Kojima, H.; Nakatsubo, N.; Kikuchi, K.; Kawahara, S.; Kirino, Y.; Nagoshi, H.; Hirata, Y.; Nagano, T. *Anal. Chem.* **1998**, *70*, 2446.
(6) Heiduschka, P.; Thanos, S. *NeuroReport* **1998**, *9*, 4051.
(7) Meineke, P.; Rauen, U.; de Groot, H.; Korth, H.-G.; Sustmann, R. *Chem.—Eur. J.* **1999**, *5*, 1738.
(8) Kojima, H.; Hirotani, M.; Nakatsubo, N.; Kikuchi, K.; Urano, Y.; Higuchi, T.; Hirata, Y.; Nagano, T. *Anal. Chem.* **2001**, *73*, 1967.
(9) Gabe, Y.; Urano, Y.; Kikuchi, K.; Kojima, H.; Nagano, T. *J. Am. Chem. Soc.* **2004**, *126*, 3357.
(10) Sasaki, E.; Kojima, H.; Nishimatsu, H.; Urano, Y.; Kikuchi, K.; Hirata, Y.; Nagano, T. *J. Am. Chem. Soc.* **2005**, *127*, 3684.
(11) Lim, M. H.; Xu, D.; Lippard, S. J. *Nat. Chem. Biol.* **2006**, *2*, 375.
(12) Lim, M. H.; Wong, B. A.; Pitcock, W. H., Jr.; Mokshagundam, D.; Baik, M.-H.; Lippard, S. J. *J. Am. Chem. Soc.* **2006**, *128*, 14363.
(13) Zheng, H.; Shang, G.-Q.; Yang, S.-Y.; Gao, X.; Xu, J.-G. *Org. Lett.* **2008**, *10*, 2357.
(14) Wang, S.; Han, M.-Y.; Huang, D. *J. Am. Chem. Soc.* **2009**, *131*, 11692.
(15) Kim, J.-H.; Heller, D. A.; Barone, P. W.; Song, C.; Zhang, J.; Trudel, L. J.; Wogan, G. N.; Tannenbaum, S. R.; Strano, M. S. *Nat. Chem.* **2009**, *1*, 473.
(16) Jourd'heuil, D. *Free Radical Biol. Med.* **2002**, *33*, 676.
(17) Roychowdhury, S.; Luthe, A.; Keilhoff, G.; Wolf, G.; Horn, T. F. W. *Glia* **2002**, *38*, 103.
(18) Wardman, P. *Free Radical Biol. Med.* **2007**, *43*, 995.
(19) Zhang, X.; Kim, W. S.; Hatcher, N.; Potgieter, K.; Moroz, L. L.; Gillette, R.; Sweedler, J. V. *J. Biol. Chem.* **2002**, *277*, 48472.
(20) Ye, X.; Rubakhin, S. S.; Sweedler, J. V. *J. Neurosci. Methods* **2008**, *168*, 373.
(21) Lim, M. H.; Lippard, S. J. *Acc. Chem. Res.* **2007**, *40*, 41.
(22) Hartung, J. *Chem. Rev.* **2009**, *109*, 4500.
(23) Lee, S. C.; Dickson, D. W.; Liu, W.; Brosnan, C. F. *J. Neuroimmunol.* **1993**, *46*, 19.
(24) Liu, B.; Neufeld, A. H. *Glia* **2000**, *30*, 178.
(25) Zhao, M. L.; Liu, J. S. H.; He, D.; Dickson, D. W.; Lee, S. C. *Brain Res.* **1998**, *813*, 402.

JA1040013